Eur. Phys. J. C (2016) 76:102
DOI 10.1140/epjc/s10052-016-3936-9

THE EUROPEAN PHYSICAL JOURNAL C

Regular Article - Theoretical Physics

Partial wave analysis of the Dirac fermions scattered from Schwarzschild black holes

Ion I. Cotăescu[a], **Cosmin Crucean**[b], **Ciprian A. Sporea**[c]

West University of Timişoara, V. Pârvan Ave. 4, 300223 Timişoara, Romania

Received: 15 July 2015 / Accepted: 5 February 2016 / Published online: 26 February 2016

Abstract Asymptotic analytic solutions of the Dirac equation, giving the scattering modes (of the continuous energy spectrum, $E > mc^2$) in Schwarzschild's chart and Cartesian gauge, are used for building the partial wave analysis of Dirac fermions scattered by black holes. In this framework, the analytic expressions of the differential cross section and induced polarization degree are derived in terms of scattering angle, mass of the black hole, and energy and mass of the fermion. Moreover, the closed form of the absorption cross section due to the scattering modes is derived showing that in the high-energy limit this tends to the event horizon area regardless of the fermion mass (including zero). A graphical study presents the differential cross section analyzing the forward/backward scattering (known also as glory scattering) and the polarization degree as functions of scattering angle. The graphical analysis shows the presence of oscillations in scattering intensity around forward/backward directions, phenomena known as spiral scattering. The energy dependence of the differential cross section is also established by using analytical and graphical methods.

1 Introduction

The complex problem of the quantum particles scattered from black holes was studied extensively, mainly considering massless scalar [1–16] or other massless boson fields [17–19], since the equations of massive fields cannot be solved analytically in the Schwarzschild geometry. This is one of the reasons why the scattering of massive Dirac fermions by black holes was studied either in particular cases [20,21] or by using combined analytical and numerical methods [22–26]. Thus in Refs. [25,26] such methods were applied for investigating the absorption cross section, the scattering intensity (pointing out the glory and spiral scattering) and the polarization degree of these scattering processes. However, in the case of the interactions of quantum particles with black holes the numerical methods may represent a difficult task since one must combine quantities at quantum scale (mass, energy of the fermion) with quantities at galactic scale (as the black hole mass). Therefore, it is obvious that any new analytic study may improve this investigation, helping us to understand the quantum mechanisms governing the scattering process.

For this reason we would like to propose in this paper the partial wave analysis of the Dirac fermions scattered from Schwarzschild black holes constructed applying exclusively analytical methods. In order to do this, we exploit the analytical properties of the (approximative) asymptotic solutions of the Dirac equation we have found some time ago [27]. These solutions were obtained in the chart with Schwarzschild coordinates where we considered the Cartesian gauge that preserves the global central symmetry of the field equations [28], allowing the separation of spherical variables just as in the central problems of special relativity [29]. We note that thanks to this gauge one of us (IIC) succeeded to solve analytically the Dirac equation on the central charts of the de Sitter and anti-de Sitter spacetimes [30–33]. In the case of the Schwarzschild chart and Cartesian gauge, after the separation of the angular variables, we remain with a pair of simple radial equations depending only on the gauge field components, which can be approximatively solved by using the Novikov radial coordinate [34,35]. We obtained thus the asymptotic radial solutions that are either of scattering type or even possible bound states [27]. However, these last mentioned states are less studied and seem to be unstable [36], so that we restrict ourselves to considering only the scattering solutions (with $E > mc^2$) for performing the partial wave analysis of the Dirac fermions scattered from black holes.

In general, when one considers the analytic expressions of the scattering quantum modes, one must impose suitable boundary conditions (in the origin or at the event horizon) in

[a] e-mail: cota@physics.uvt.ro
[b] e-mail: crucean@physics.uvt.ro
[c] e-mail: ciprian.sporea89@e-uvt.ro

order to fix the integration constants determining the asymptotic behavior and implicitly the phase shifts of the partial wave analysis. Having here only the asymptotic form of the Dirac spinors in the black hole field we must replace the boundary conditions with suitable *asymptotic* conditions playing the same role in determining the integration constants of our asymptotic solutions. Fortunately, this can be done assuming that for large values of the angular momentum the collision becomes elastic approaching the Newtonian limit [20,21]. This hypothesis is enough for determining completely the integration constants and deriving the analytical forms of the phase shifts, scattering amplitudes, differential cross section, and polarization degree. The nice surprise is that this approach emphasizes the absorption of the fermions by black holes in a natural manner, laying out the absorption cross section in an analytical closed form with some associated selection rules.

The paper is organized as follows. In Sect. 2 we briefly present our method of separating the variables of the Dirac equation on central backgrounds and Cartesian gauge focusing on the mentioned approximative solutions of the Dirac equation in Schwarzschild's charts, corresponding to the continuous energy spectrum [27]. Section 3 is devoted to our partial wave analysis based on the asymptotic condition (discussed in Appendix C), which fixes the integration constants giving the analytical form of the phase shifts encapsulating both cases studied here, the elastic scattering of fermions and their absorption by a black hole. We verify that our scattering amplitudes have the correct Newtonian limit and we derive the scattering intensity and polarization degree. Special attention is paid to the absorption cross section, for which we give the analytic expression of the partial cross sections and the selection rules indicating in which partial wave we can find absorption. Section 4 is devoted to the graphical analysis and discussion of the physical consequences of our results. Here we show that our analytical results concerning the elastic scattering are very similar to those obtained by using analytical–numerical methods [25,26], but there are some differences as concerns the absorption. Other conclusions are summarized in the last section.

In the following we use natural units with $c = \hbar = G = 1$.

2 Approximating Dirac spinors in Schwarzschild's geometry

The Dirac equation in curved spacetimes is defined in frames $\{x; e\}$ formed by a local chart of coordinates x^μ, labeled by natural indices, $\alpha, \ldots, \mu, \nu, \ldots = 0, 1, 2, 3$, and an orthogonal local frame and coframe defined by the gauge fields (or tetrads), $e_{\hat\alpha}$, respectively, $\hat e^{\hat\alpha}$, labeled by the local indices $\hat\alpha, \ldots, \hat\mu, \ldots$ with the same range.

In locally Minkowskian manifolds (M, g), having as a flat model the Minkowski spacetime (M_0, η) of the metric $\eta = \mathrm{diag}(1, -1, -1, -1)$, the gauge fields satisfy the usual duality conditions, $\hat e^{\hat\mu}_\alpha\, e^\alpha_{\hat\nu} = \delta^{\hat\mu}_{\hat\nu}$, $\hat e^{\hat\mu}_\alpha\, e^\beta_{\hat\mu} = \delta^\beta_\alpha$ and the orthogonality relations, $e_{\hat\mu}\cdot e_{\hat\nu} = \eta_{\hat\mu\hat\nu}$, $\hat e^{\hat\mu}\cdot\hat e^{\hat\nu} = \eta^{\hat\mu\hat\nu}$. The gauge fields define the local derivatives $\hat\partial_{\hat\mu} = e^\nu_{\hat\mu}\partial_\nu$ and the 1-forms $\omega^{\hat\mu} = \hat e^{\hat\mu}_\nu \mathrm{d}x^\nu$ giving the line element $\mathrm{d}s^2 = \eta_{\hat\alpha\hat\beta}\omega^{\hat\alpha}\omega^{\hat\beta} = g_{\mu\nu}\mathrm{d}x^\mu\mathrm{d}x^\nu$ (with $g_{\mu\nu} = \eta_{\hat\alpha\hat\beta}\hat e^{\hat\alpha}_\mu \hat e^{\hat\beta}_\nu$).

2.1 The Dirac equation in central charts and Cartesian gauge

In a given frame $\{x; e\}$, the Dirac equation of a free spinor field ψ of mass m has the form

$$i\gamma^{\hat\alpha} D_{\hat\alpha}\psi - m\psi = 0, \tag{1}$$

where $\gamma^{\hat\alpha}$ are the point-independent Dirac matrices that satisfy $\{\gamma^{\hat\alpha}, \gamma^{\hat\beta}\} = 2\eta^{\hat\alpha\hat\beta}$ and define the generators of the spinor representation of the $SL(2, C)$ group, $S^{\hat\alpha\hat\beta} = \frac{i}{4}[\gamma^{\hat\alpha}, \gamma^{\hat\beta}]$, which give the spin connections of the covariant derivatives,

$$D_{\hat\alpha} = e^\mu_{\hat\alpha} D_\mu = \hat\partial_{\hat\alpha} + \frac{i}{2} S^{\hat\beta\hat\gamma}_{\cdot\cdot} \hat\Gamma^{\hat\gamma}_{\hat\alpha\hat\beta}, \tag{2}$$

depending on the connection components in local frames $\hat\Gamma^{\hat\delta}_{\hat\mu\hat\nu} = e^\alpha_{\hat\mu} e^\beta_{\hat\nu}(\hat e^{\hat\delta}_\gamma \Gamma^\gamma_{\alpha\beta} - \hat e^{\hat\delta}_{\beta,\alpha})$ where the notation $\Gamma^\gamma_{\alpha\beta}$ stands for the usual Christoffel symbols.

In this approach the Dirac equation (1) takes the explicit form

$$i\gamma^{\hat\alpha} e^\mu_{\hat\alpha}\partial_\mu\psi - m\psi + \frac{i}{2}\frac{1}{\sqrt{-g}}\partial_\mu(\sqrt{-g}e^\mu_{\hat\alpha})\gamma^{\hat\alpha}\psi - \frac{1}{4}\{\gamma^{\hat\alpha}, S^{\hat\beta\hat\gamma}_{\cdot\cdot}\}\hat\Gamma^{\hat\gamma}_{\hat\alpha\hat\beta}\psi = 0, \tag{3}$$

where $g = \det(g_{\mu\nu})$. Moreover, from the conservation of the electric charge, one deduces that the time-independent relativistic scalar product of two spinors [30]

$$(\psi, \psi') = \int_D \mathrm{d}^3x\sqrt{-g(x)}\, e^0_{\hat\mu}(x)\bar\psi(x)\gamma^{\hat\mu}\psi'(x), \tag{4}$$

is given by the integral over the space domain D of the local chart under consideration.

In general, a manifold with central symmetry has a static central chart with spherical coordinates (t, r, θ, ϕ), associated to the Cartesian ones $(t, \vec x)$, with $r = |\vec x|$, covering the space domain $D = D_r \times S^2$, i.e. $r \in D_r$ while θ and ϕ cover the sphere S^2. The form of the Dirac equation in any chart is strongly dependent on the choice of the tetrad gauge. For this reason, our approach is based on the virtues of the mentioned Cartesian gauge which is defined by the 1-forms [28,30],

$$\omega^0 = w(r)\mathrm{d}t, \tag{5}$$

$$\omega^1 = \frac{w(r)}{u(r)}\sin\theta\cos\phi\,\mathrm{d}r + \frac{rw(r)}{v(r)}\cos\theta\cos\phi\,\mathrm{d}\theta - \frac{rw(r)}{v(r)}\sin\theta\sin\phi\,\mathrm{d}\phi\,, \tag{6}$$

$$\omega^2 = \frac{w(r)}{u(r)}\sin\theta\sin\phi\,\mathrm{d}r + \frac{rw(r)}{v(r)}\cos\theta\sin\phi\,\mathrm{d}\theta + \frac{rw(r)}{v(r)}\sin\theta\cos\phi\,\mathrm{d}\phi\,, \tag{7}$$

$$\omega^3 = \frac{w(r)}{u(r)}\cos\theta\,\mathrm{d}r - \frac{rw(r)}{v(r)}\sin\theta\,\mathrm{d}\theta, \tag{8}$$

expressed in terms of three arbitrary functions of r, denoted by u, v, and w, which allow us to write the general line element

$$\mathrm{d}s^2 = \eta_{\hat{\alpha}\hat{\beta}}\omega^{\hat{\alpha}}\omega^{\hat{\beta}} = w(r)^2\left[\mathrm{d}t^2 - \frac{\mathrm{d}r^2}{u(r)^2} - \frac{r^2}{v(r)^2}(\mathrm{d}\theta^2 + \sin^2\theta\mathrm{d}\phi^2)\right]. \tag{9}$$

We have shown that in this gauge the last term of Eq. (3) does not contribute and, moreover, there is a simple transformation, $\psi \to vw^{-\frac{3}{2}}\psi$, able to eliminate the terms containing the derivatives of the functions u, v, and w, leading thus to a simpler *reduced* Dirac equation [30]. The advantage of this equation is that its spherical variables can be separated just as in the case of the central problems in Minkowski spacetime [29]. Consequently, the Dirac field can be written as a linear combination of particular solutions of given energy, E. Those of positive frequency,

$$U_{E,\kappa,m_j}(x) = U_{E,\kappa,m_j}(t,r,\theta,\phi) = \frac{v(r)}{rw(r)^{3/2}}\left[f^+_{E,\kappa}(r)\Phi^+_{m_j,\kappa}(\theta,\phi) + f^-_{E,\kappa}(r)\Phi^-_{m_j,\kappa}(\theta,\phi)\right]e^{-iEt}, \tag{10}$$

are particle-like energy eigenspinors expressed in terms of radial wave functions, $f^{\pm}_{E,\kappa}$, and usual four-component angular spinors $\Phi^{\pm}_{m_j,\kappa}$ [29]. It is well known that these spinors are orthogonal to each other, being labeled by the angular quantum numbers m_j and

$$\kappa = \begin{cases} j+\frac{1}{2} = l & \text{for} \quad j = l-\frac{1}{2}, \\ -(j+\frac{1}{2}) = -l-1 & \text{for} \quad j = l+\frac{1}{2}, \end{cases} \tag{11}$$

which encapsulates the information as regards the quantum numbers l and $j = l \pm \frac{1}{2}$ as defined in Refs. [29,37] (while in Ref. [26] κ is of opposite sign). The spherical spinors are normalized to unity with respect to their own angular scalar product. We note that the antiparticle-like energy eigenspinors can be obtained directly using the charge conjugation as in the flat case [39].

Thus the problem of the angular motion is completely solved for any central background. We are left with a pair of radial wave functions, $f^{\pm}$ (denoted from now on without indices), which satisfy two radial equations that can be written in compact form as the eigenvalue problem $H_r\mathcal{F} = E\mathcal{F}$ of the radial Hamiltonian [30],

$$H_r = \begin{pmatrix} m\,w(r) & -u(r)\frac{\mathrm{d}}{\mathrm{d}r} + \kappa\frac{v(r)}{r} \\ u(r)\frac{\mathrm{d}}{\mathrm{d}r} + \kappa\frac{v(r)}{r} & -m\,w(r) \end{pmatrix}, \tag{12}$$

in the space of two-component vectors (or doublets), $\mathcal{F} = (f^+, f^-)^T$, equipped with the radial scalar product [30]

$$(\mathcal{F},\mathcal{F}') = \langle U, U'\rangle = \int_{D_r}\frac{\mathrm{d}r}{u(r)}\,\mathcal{F}^\dagger\mathcal{F}', \tag{13}$$

resulting from the general formula (4) where we have to take $\sqrt{-g(x)} = \frac{w(r)^4}{u(r)v(r)^2}r^2\sin\theta$, the spinors U and U' of the form (10) and $e^0_{\hat{\mu}}\gamma^{\hat{\mu}} = \frac{1}{w(r)}\gamma^0$. This scalar product has to select the 'good' radial wave functions, i.e. tempered distributions, which enter in the structure of the particle-like energy eigenspinors.

In the central charts each particular solution (10) gives rise to a *partial* radial current defined as

$$J_{\mathrm{rad}} = \int_{S^2}\mathrm{d}\theta\,\mathrm{d}\phi\sqrt{-g(x)}\,\overline{U}(x)\gamma_{\mathrm{rad}}U(x), \tag{14}$$

where we take into account that in our Cartesian gauge we have

$$\gamma_{\mathrm{rad}} = e^r_{\hat{\mu}}\gamma^{\hat{\mu}} = \frac{u(r)}{w(r)}\gamma_x, \quad \gamma_x = \frac{1}{r}\,\vec{x}\cdot\vec{\gamma}. \tag{15}$$

Exploiting then the property $\gamma^0\gamma_x\Phi^{\pm} = \pm i\Phi^{\mp}$ and the orthogonality of the spherical spinors [29] we obtain the final result

$$J_{\mathrm{rad}} = i\left(f^+f^{-*} - f^{+*}f^-\right). \tag{16}$$

Now it is obvious that these currents are conserved and independent on r, since $\partial_r J_{\mathrm{rad}} = 0$ whenever the functions $f^{\pm}$ satisfy the above radial equations. These will represent useful significant constants of motion in the scattering process.

2.2 Analytic asymptotic solutions in Scwarzschild's charts with Cartesian gauge

Let us assume that a Dirac particle of mass m is moving freely (as a perturbation) in the central gravitational field of a black hole of mass M with the Schwarzschild line element

$$ds^2 = \left(1 - \frac{r_0}{r}\right) dt^2 - \frac{dr^2}{1 - \frac{r_0}{r}} - r^2(d\theta^2 + \sin^2\theta\, d\phi^2), \tag{17}$$

defined on the radial domain $D_r = (r_0, \infty)$ where $r_0 = 2M$. Hereby we identify the functions

$$u(r) = 1 - \frac{r_0}{r}, \quad v(r) = w(r) = \sqrt{1 - \frac{r_0}{r}}, \tag{18}$$

which give the radial Hamiltonian (12). The resulting radial problem cannot be solved analytically as it stays forcing one to resort to numerical methods [26] or to some approximations.

In Ref. [27] we proposed an effective method of approximating this radial problem expanding the radial equations in terms of the Novikov dimensionless coordinate [34,35],

$$x = \sqrt{\frac{r}{r_0} - 1} \in (0, \infty). \tag{19}$$

Using this new variable and introducing the notations

$$\mu = r_0 m, \quad \epsilon = r_0 E, \tag{20}$$

we rewrite the exact radial problem as

$$\begin{pmatrix} \mu\sqrt{1+x^2} - \epsilon\left(x + \frac{1}{x}\right) & -\frac{1}{2}\frac{d}{dx} + \frac{\kappa}{\sqrt{1+x^2}} \\ \frac{1}{2}\frac{d}{dx} + \frac{\kappa}{\sqrt{1+x^2}} & -\mu\sqrt{1+x^2} - \epsilon\left(x + \frac{1}{x}\right) \end{pmatrix} \times \begin{pmatrix} f^+(x) \\ f^-(x) \end{pmatrix} = 0. \tag{21}$$

Moreover, from Eq. (13) we find that the radial scalar product now takes the form

$$(\mathcal{F}_1, \mathcal{F}_2) = 2r_0 \int_0^\infty dx \left(x + \frac{1}{x}\right) \mathcal{F}_1^\dagger \mathcal{F}_2. \tag{22}$$

We note that the singular form above, due to our special parametrization and use of the Novikov variable, is merely apparent, since this comes from the usual regular scalar product (4). Moreover, we have shown that there exist square integrable spinors with respect to this scalar product [27].

For very large values of x, we can use the Taylor expansion with respect to $\frac{1}{x}$ of the operator (21) neglecting the terms of the order $O(1/x^2)$. We obtain thus the *asymptotic* radial problem [27], which can be rewritten as

$$\begin{pmatrix} \frac{1}{2}\frac{d}{dx} + \frac{\kappa}{x} & -\mu\left(x + \frac{1}{2x}\right) - \epsilon\left(x + \frac{1}{x}\right) \\ -\mu\left(x + \frac{1}{2x}\right) + \epsilon\left(x + \frac{1}{x}\right) & \frac{1}{2}\frac{d}{dx} - \frac{\kappa}{x} \end{pmatrix} \times \begin{pmatrix} f^+(x) \\ f^-(x) \end{pmatrix} = 0, \tag{23}$$

after reversing between themselves the lines of the matrix operator. This is necessary for diagonalizing simultaneously the term containing derivatives and the one proportional to x, as in the Dirac–Coulomb case [37]. This can be done by using the matrix

$$T = \begin{vmatrix} -i\sqrt{\mu+\epsilon} & i\sqrt{\mu+\epsilon} \\ \sqrt{\epsilon-\mu} & \sqrt{\epsilon-\mu} \end{vmatrix}, \tag{24}$$

for transforming the radial doublet as $\mathcal{F} \to \hat{\mathcal{F}} = T^{-1}\mathcal{F} = (\hat{f}^+, \hat{f}^-)^T$, obtaining the new system of radial equations

$$\left[\frac{1}{2}x\frac{d}{dx} \pm i\left(\frac{\mu^2 - 2\epsilon^2}{2\nu} - \nu x^2\right)\right] \hat{f}^\pm = \left(\kappa \mp \frac{i\epsilon\mu}{2\nu}\right) \hat{f}^\mp, \tag{25}$$

where $\nu = \sqrt{\epsilon^2 - \mu^2}$. These equations can be solved analytically for any values of ϵ. In Ref. [27] we derived the spinors corresponding to the continuous spectrum $\epsilon \in [\mu, \infty)$, but without investigating scattering effects.

Here we would like to complete this study by calculating the fermion scattering amplitudes starting with the asymptotic solutions of Ref. [27] we briefly present below. The radial equations (25) can be analytically solved for the continuous energy spectrum, $\epsilon > \mu$, in terms of the Whittaker functions as [27]

$$\hat{f}^+(x) = C_1^+ \frac{1}{x} M_{r_+,s}(2i\nu x^2) + C_2^+ \frac{1}{x} W_{r_+,s}(2i\nu x^2), \tag{26}$$

$$\hat{f}^-(x) = C_1^- \frac{1}{x} M_{r_-,s}(2i\nu x^2) + C_2^- \frac{1}{x} W_{r_-,s}(2i\nu x^2), \tag{27}$$

where we denote

$$s = \sqrt{\kappa^2 + \frac{\mu^2}{4} - \epsilon^2}, \quad r_\pm = \mp\frac{1}{2} - iq, \quad q = \nu + \frac{\mu^2}{2\nu}. \tag{28}$$

The integration constants must satisfy [27]

$$\frac{C_1^-}{C_1^+} = \frac{s - iq}{\kappa - i\lambda}, \quad \frac{C_2^-}{C_2^+} = -\frac{1}{\kappa - i\lambda}, \quad \lambda = \frac{\epsilon\mu}{2\nu}. \tag{29}$$

We observe that these solutions are similar to those of the relativistic Dirac–Coulomb problem. The functions $M_{r_\pm,s}(2i\nu x^2) = (2i\nu x^2)^{s+\frac{1}{2}}[1 + O(x^2)]$ are regular in $x = 0$, where the functions $W_{r_\pm,s}(2i\nu x^2)$ diverge as x^{1-2s} if $s > \frac{1}{2}$ [40]. These solutions will help us to find the scattering amplitudes of the Dirac particles by black holes, after fixing the integration constants.

3 Partial wave analysis

We consider now the scattering of Dirac fermions on a black hole. This is described by the energy eigenspinor U whose asymptotic form,

$$U \to U_{\text{plane}}(\vec{p}) + A(\vec{p},\vec{n})U_{\text{sph}}, \tag{30}$$

for $r \to \infty$ (where the gravitational field vanishes) is given by the plane wave spinor of momentum $\vec{p}$ and the free spherical spinors of the flat case behaving as

$$U_{\text{sph}} \propto \frac{1}{r}\, e^{ipr - iEt}, \quad p = \sqrt{E^2 - m^2} = \frac{\nu}{r_0}. \tag{31}$$

Here we fix the geometry such that $\vec{p} = p\vec{e}_3$, while the direction of the scattered fermion is given by the scattering angles θ and ϕ, which are just the spheric angles of the unit vector $\vec{n}$. Then the scattering amplitude

$$A(\vec{p},\vec{n}) = f(\theta) + ig(\theta)\frac{\vec{p}\wedge\vec{n}}{|\vec{p}\wedge\vec{n}|}\cdot\vec{\sigma} \tag{32}$$

depends on two scalar amplitudes, $f(\theta)$ and $g(\theta)$, which can be studied by using partial wave analysis.

3.1 Asymptotic conditions and phase shifts

The partial wave analysis exploits the asymptotic form of the exact analytic solutions which satisfy suitable boundary conditions that in our case might be fixed at the event horizon (where $x = 0$). Unfortunately, we have here only the asymptotic solutions (26) and (27) whose integration constants cannot be related to those of the approximative solutions near event horizon [27] without resorting to numerical methods [20–26]. Therefore, as long as we restrict ourselves only to an analytical study, we cannot match boundary conditions near the event horizon, being forced to find suitable asymptotic conditions for determining the integration constants. Then the behavior near horizon can be discussed, a posteriori, focusing on the partial radial currents and especially on the absorption cross section, which can easily be derived in our approach.

When the Dirac fermions are scattered from the central potentials, the particular spinors of the parameters (p,κ) represent partial waves having the asymptotic form

$$\mathcal{F} \propto \begin{matrix}\sqrt{E+m}\sin\\ \sqrt{E-m}\cos\end{matrix}\left(pr - \frac{\pi l}{2} + \delta_\kappa\right), \tag{33}$$

where the phase shifts δ_κ can be, in general, complex numbers which allow one to write down the amplitudes in terms of the Lagrange polynomials of $\cos\theta$. Each partial wave gives rise to the radial current (16), which can be put now in the form

$$J_{\text{rad}}(p,\kappa) \propto -p\sinh(2\Im\delta_\kappa). \tag{34}$$

The scattering is elastic when the phase shifts δ_κ are real numbers such that the partial radial currents vanish. Whenever there are inelastic processes the phase shifts become complex numbers, whose imaginary parts are related to the inelastic behavior, producing the non-vanishing radial currents indicating absorption.

In Appendix C we show that in our approach it is necessary to adopt the general asymptotic condition $C_2^+ = C_2^- = 0$ in order to have *elastic* collisions with a correct Newtonian limit for large angular momentum. It is remarkable that this asymptotic condition selects the asymptotic spinors that are regular in $x = 0$; but this cannot be interpreted as a boundary condition since the exact solutions have a different structure near the event horizon [27].

Under such circumstances we have to use the asymptotic forms of the radial functions for large x resulting from Eq. (A2). We observe that the first term from (A2) is dominant for $\hat{f}^+$, while the second term in (A2) is dominant for $\hat{f}^-$, such that for $x \to \infty$ the radial functions behave as

$$\hat{f}^+(x) \to C_1^+ e^{-\frac{1}{2}\pi q}\frac{\Gamma(2s+1)}{\Gamma(1+s+iq)}\, e^{i[\nu x^2 + q\ln(2\nu x^2)]}, \tag{35}$$

$$\hat{f}^-(x) \to C_1^- e^{-\frac{1}{2}\pi q}\frac{\Gamma(2s+1)}{\Gamma(1+s-iq)}\, e^{-i[\nu x^2 + \pi s + q\ln(2\nu x^2)]}. \tag{36}$$

Hereby we derive the asymptotic form (33) of the doublet $\mathcal{F} = T\hat{\mathcal{F}}$ observing that the argument of the trigonometric functions can be deduced as $\frac{1}{2}\arg\left(\frac{\hat{f}^+}{\hat{f}^-}\right)$. Then by using Eq. (29a) and taking into account that Eqs. (19) and (31b) allow us to replace $\nu x^2 = p(r - r_0)$, we obtain the definitive asymptotic form of the radial functions for the scattering by black holes,

$$\begin{aligned}\mathcal{F} &= \begin{pmatrix} i\sqrt{\epsilon+\mu}\,(\hat{f}^- - \hat{f}^+)\\ \sqrt{\epsilon-\mu}\,(\hat{f}^+ + \hat{f}^-)\end{pmatrix}\\ &\propto \begin{matrix}\sqrt{E+m}\sin\\ \sqrt{E-m}\cos\end{matrix}\left(pr - \frac{\pi l}{2} + \delta_\kappa + \vartheta(r)\right),\end{aligned} \tag{37}$$

whose point-independent phase shifts δ_κ give the quantities

$$S_\kappa = e^{2i\delta_\kappa} = \left(\frac{\kappa - i\lambda}{s - iq}\right)\frac{\Gamma(1+s-iq)}{\Gamma(1+s+iq)}e^{i\pi(l-s)}. \tag{38}$$

Notice that the values of κ and l are related as in Eq. (11), i.e. $l = |\kappa| - \frac{1}{2}(1 - \operatorname{sign}\kappa)$. The remaining radially dependent phase,

$$\vartheta(r) = -pr_0 + q\ln[2p(r - r_0)], \tag{39}$$

which does not depend on angular quantum numbers, may be ignored as in the Dirac–Coulomb case [26,37].

We arrived thus at the final result (38) depending on the parameters introduced above, which can be expressed in terms of physical quantities by using Eq. (31b) as

$$s=\sqrt{\kappa^2-k^2},\quad k=M\sqrt{4p^2+3m^2}, \tag{40}$$

$$q=\frac{M}{p}(2p^2+m^2), \tag{41}$$

$$\lambda=\frac{M}{p}m\sqrt{m^2+p^2}. \tag{42}$$

The parameters $k,q,\lambda\in\mathbb{R}^+$ are positively defined and satisfy the identity

$$k^2=q^2-\lambda^2. \tag{43}$$

In the particular case of the massless fermions ($m=0$) we are left with the unique parameter $k=q=2pM$, since $\lambda=0$.

The parameter s has a special position since this can take either real values or pure imaginary ones. Let us briefly discuss these two cases.

The case of elastic scattering arises for the values of κ (at given p) that satisfy the condition

$$|\kappa|\geq n+1, \tag{44}$$

where $n=\text{floor}(k)$ is the largest integer less than k. Then $s=\sqrt{\kappa^2-k^2}\in\mathbb{R}$ and the identity (43) guarantees that the phase shifts of Eq. (38) are real numbers such that $|S_\kappa|=1$.

The case of absorption is present in the partial waves for which we have

$$1\leq|\kappa|\leq n. \tag{45}$$

Here we meet a branch point in $s=0$ and two solutions $s=\pm i|s|=\pm i\sqrt{k^2-\kappa^2}$; among them we must choose $s=-i|s|$, since only in this manner we select the physical case of $|S_\kappa|<1$. More specific, by substituting $s=-i|s|$ in Eq. (38) we obtain the simple closed form

$$|S_\kappa|=|S_{-\kappa}|=e^{-2\Im\delta_\kappa}=e^{-\pi|s|}\sqrt{\frac{\sinh\pi(q-|s|)}{\sinh\pi(q+|s|)}} \tag{46}$$

showing that $0<|S_\kappa|<1$, since $|s|<q$ for any (p,κ) obeying the condition (45). Moreover, we can verify that in the limit of the large momentum (or energy) the absorption tends to become maximal, since

$$\lim_{p\to\infty}|S_\kappa|=0, \tag{47}$$

regardless of the fermion mass.

Finally, we note that for any values of the above parameters the phase shifts δ_l and δ_{-l} are related as

$$e^{2i(\delta_l-\delta_{-l})}=\frac{pl-imM\sqrt{p^2+m^2}}{pl+imM\sqrt{p^2+m^2}}, \tag{48}$$

which means that for massless Dirac fermions we have $\delta_l=\delta_{-l}$.

This is the basic framework of the relativistic partial wave analysis of the Dirac fermions scattered by Schwarzschild black holes in which we consider exclusively the contribution of the scattering modes. Our results are in accordance with the Newtonian limit since in the large-l limits and for very small momentum we can take $s\sim|\kappa|\sim l$ and $\lambda\sim q$ such that our phase shifts (38) become just the Newtonian ones, Eq. (B1) [20,21].

On the other hand, we observe that our phase shifts are given by a formula which has the same form as that deduced for the Dirac–Coulomb scattering [37]. Indeed, by replacing in Eq. (38) the parameters

$$s\to\sqrt{\kappa^2-Z^2\alpha^2},\quad q\to\frac{Z\alpha}{p}E,\quad \lambda\to\frac{Z\alpha}{p}m, \tag{49}$$

we recover the phase shifts of the Dirac–Coulomb scattering. However, there are significant differences between these parameterizations showing that these two systems are of different natures.

3.2 Partial amplitudes and cross sections

Now we have all the elements for calculating the analytic expressions of the amplitudes and cross sections in terms of the phase shifts defined by Eq. (38). In the relativistic theory, the scalar amplitudes of Eq. (32),

$$f(\theta)=\sum_{l=0}^{\infty}a_l\,P_l(\cos\theta), \tag{50}$$

$$g(\theta)=\sum_{l=1}^{\infty}b_l\,P_l^1(\cos\theta), \tag{51}$$

depend on the following *partial* amplitudes [26,37],

$$a_l=(2l+1)f_l=\frac{1}{2ip}\left[(l+1)(S_{-l-1}-1)+l(S_l-1)\right], \tag{52}$$

$$b_l=(2l+1)g_l=\frac{1}{2ip}\left(S_{-l-1}-S_l\right). \tag{53}$$

In our problem the quantities S_κ are given by the analytic expression (38) such that we can apply analytic methods for studying the above amplitudes, which give the *elastic* scattering intensity or the differential cross section,

$$\frac{\mathrm{d}\sigma}{\mathrm{d}\Omega} = |f(\theta)|^2 + |g(\theta)|^2, \tag{54}$$

and the polarization degree,

$$\mathcal{P}(\theta) = -i\frac{f(\theta)^* g(\theta) - f(\theta) g(\theta)^*}{|f(\theta)|^2 + |g(\theta)|^2}. \tag{55}$$

This last quantity is interesting for the scattering of massive fermions representing the induced polarization for an unpolarized initial beam.

Let us verify first that our approach recovers the correct Newtonian limit in weak gravitational fields (with small M) where the partial amplitudes can be expanded as

$$f_l = M f_l^{(1)} + M^2 f_l^{(2)} + \cdots \quad l = 0, 1, 2, \ldots, \tag{56}$$

$$g_l = M g_l^{(1)} + M^2 g_l^{(2)} + \cdots \quad l = 1, 2, \ldots. \tag{57}$$

Our algebraic codes indicate that the cases $l = 0$ and $l > 0$ must be studied separately since the expansion of f_l does not commute with its limit for $l \to 0$. However, this is not surprising since a similar phenomenon can be met in the Dirac–Coulomb problem. Then, according to Eqs. (52), (53), and (38), we obtain first the expansion for $l = 0$,

$$f_0^{(1)} = \gamma\frac{2p^2+m^2}{p^2} - \frac{2p^2+m^2-m\sqrt{p^2+m^2}}{2p^2}, \tag{58}$$

$$\begin{aligned} f_0^{(2)} = {} & i\gamma^2\frac{(2p^2+m^2)^2}{p^3} - i\gamma\frac{2p^2+m^2}{p^3} \\ & \times\left(2p^2+m^2-m\sqrt{p^2+m^2}\right) \\ & -i\frac{m(2p^2+m^2)}{2p^3}\sqrt{p^2+m^2} \\ & +i\frac{4p^4+5p^2m^2+2m^4}{4p^3} + \pi\frac{4p^2+3m^2}{4p}, \end{aligned} \tag{59}$$

where γ is the Euler constant. Furthermore, for any $l > 0$ we find the terms of first order,

$$f_l^{(1)} = -\psi(l+1)\frac{2p^2+m^2}{p^2}, \tag{60}$$

$$g_l^{(1)} = -\frac{1}{2l(l+1)}\frac{2p^2+m^2-m\sqrt{p^2+m^2}}{p^2}, \tag{61}$$

depending on the digamma function ψ, and the more complicated ones of second order,

$$\begin{aligned} f_l^{(2)} = {} & i\psi(l+1)^2\frac{(2p^2+m^2)^2}{p^3} \\ & -\frac{i}{2l(l+1)}\frac{m(2p^2+m^2)}{p^3}\sqrt{p^2+m^2} \\ & +\frac{i}{4l(l+1)}\frac{2m^4+5p^2m^2+4p^4}{p^3} \\ & +\frac{\pi}{2(2l+1)}\frac{4p^2+3m^2}{p}, \end{aligned} \tag{62}$$

$$\begin{aligned} g_l^{(2)} = {} & \frac{i\psi(l+1)}{l(l+1)}\frac{2p^2+m^2}{p^3}\left(2p^2+m^2-m\sqrt{p^2+m^2}\right) \\ & +\frac{i}{l^2(l+1)^2}\frac{m(2p^2+m^2)}{p^3}\sqrt{p^2+m^2} \\ & -\frac{i}{4l^2(l+1)^2}\frac{4p^4+5m^2p^2+2m^4}{p^3} \\ & -\frac{\pi}{4l(l+1)(2l+1)}\frac{4p^2+3m^2}{p}, \end{aligned} \tag{63}$$

which show the dependence on l and p. Then, from Eq. (B3) we observe that $f_l^{(1)}$ and the first term of $f_l^{(2)}$ are of Newtonian form, increasing with l because of the digamma function. The other terms decrease when l is increasing so that we verify again that our partial wave analysis has a correct Newtonian limit for large l, as happens in the well-known case of the scalar particles [20,21].

In other respects, we observe that the partial amplitudes of the massless fermions are regular in $p = 0$, while those of the massive particles diverge in any order. Thus the problem of removing the infrared catastrophe in the massive case seems to remain as a serious challenge.

Important global quantities, independent on θ, are the total cross sections. The *elastic* cross section,

$$\begin{aligned} \sigma_e &= 2\pi\int_{-1}^{1}\mathrm{d}\cos\theta\left[|f(\theta)|^2+|g(\theta)|^2\right] \\ &= 4\pi\sum_{\kappa}(2l+1)\left[|f_l|^2 + l(l+1)|g_l|^2\right] \\ &= \frac{\pi}{p^2}\sum_{\kappa}\Big\{2l+1+(l+1)|S_{-l-1}|^2 + l|S_l|^2 \\ &\quad -2\left[(l+1)\Re S_{-l-1} + l\Re S_l\right]\Big\}, \end{aligned} \tag{64}$$

is obtained by integrating the scattering intensity (54) over θ and ϕ, according to the normalization integral

$$\int_{-1}^{1}\mathrm{d}x\, P_l^m(x) P_{l'}^m(x) = \frac{2\delta_{ll'}}{2l+1}\frac{(l+m)!}{(l-m)!}. \tag{65}$$

The general expression (64) gives the elastic cross section even in the presence of absorption when $|S_\kappa| < 1$. For the genuine elastic scattering (without absorption and $|S_\kappa| = 1$), the elastic cross section σ_e represents just the total cross section σ_t such that we can write

$$\sigma_t = \frac{2\pi}{p^2}\sum_{\kappa}\left[2l+1-(l+1)\Re S_{-l-1} - l\Re S_l\right], \tag{66}$$

and one deduces that the absorption cross section, $\sigma_a = \sigma_t - \sigma_e$, reads [26]

$$\sigma_a = \frac{\pi}{p^2}\sum_{\kappa}\left[(l+1)(1-|S_{-l-1}|^2) + l(1-|S_l|^2)\right]$$

$$= \frac{2\pi}{p^2}\sum_{l=1}^{n} l(1-|S_l|^2), \tag{67}$$

since for $s=-i|s|$ we have $|S_{-\kappa}|=|S_\kappa|$ as in Eq. (46).

This last cross section deserves special attention, since this can be calculated at any time as a finite sum indicating how the fermions can be absorbed by black holes. This is a function of the momentum p since all our parameters, including n, depend on it. For this reason it is convenient to represent the absorption cross section as

$$\sigma_a = \sum_{l\geq 1}\sigma_a^l(p) \tag{68}$$

in terms of the partial cross sections whose definitive closed form,

$$\sigma_a^l(p) = \theta(k-l)\frac{2\pi l}{p^2}\left[1-e^{-2\pi\sqrt{k^2-l^2}}\,\frac{\sinh\pi(q-\sqrt{k^2-l^2})}{\sinh\pi(q+\sqrt{k^2-l^2})}\right], \tag{69}$$

is derived according to Eqs. (46) and (67), while the condition (45) introduces the Heaviside step function $\theta(k-l)$. Hereby we understand that the absorption arises in the partial wave l for the values of p satisfying the condition $k>l$. This means that for large values of l there may appear non-vanishing thresholds,

$$p_l = \begin{cases} 0 & \text{if} \quad 1\leq l\leq\sqrt{3}mM, \\ \frac{\sqrt{l^2-3m^2M^2}}{2M} & \text{if} \quad l>\sqrt{3}mM, \end{cases}, \tag{70}$$

indicating that the fermions with $|\kappa|=l$ can be absorbed by a black hole only if $p\geq p_l$. Obviously, when $\sqrt{3}mM<1$ we have $p_l\neq 0$ for any l such that we meet a non-vanishing threshold in every partial wave. This happens for massless fermions too when we have the equidistant thresholds $p_l=\frac{l}{2M}$ for any $l\geq 1$.

The existence of these thresholds is important, since these keep under control the effect of the singularities in $p=0$. Thus for any partial wave with $p_l>0$ the Heaviside function prevents the partial cross section to be singular, but when $p_l=0$ then p reaches the singularity point $p=0$, where the partial cross section diverges. Obviously, for $\sqrt{3}mM<1$ all the partial sections are finite.

Finally, we must specify that in the high-energy limit all these absorption cross sections tend to the event horizon (apparent) area, indifferent to the fermion mass $m\geq 0$, as results from Eq. (47), which yields

$$\lim_{p\to\infty}\sigma_a = \lim_{p\to\infty}\frac{2\pi}{p^2}\sum_{l=1}^{n}1 = \lim_{p\to\infty}\frac{\pi}{p^2}n(n+1)=4\pi M^2, \tag{71}$$

since $n(n+1)\sim k^2\sim 4M^2p^2$. This asymptotic value is less than the geometrical optics value of $27\pi M^2$ [38], which is the high-energy limit of the absorption cross sections obtained applying analytical–numerical methods [25,26]. The explanation could be that here we neglected the effects of possible unstable bound states [27,36] that may give rise to a resonant scattering.

4 Numerical examples

Our purpose now is to use the graphical analysis for understanding the physical consequences of our analytical results encapsulated in quite complicated formulas and the infinite series (50) and (51), which are poorly convergent or even divergent since their coefficients a_l and b_l are increasing with l faster than $l\ln l$, respectively, l^{-1}.

This is an unwanted effect of the singularity at $\theta=0$ but which can be attenuated adopting the method of Ref. [41], which consists in replacing the series (50) and (51) by the mth reduced ones,

$$f(\theta) = \frac{1}{(1-\cos\theta)^{m_1}}\sum_{l\geq 0}a_l^{(m_1)}P_l(cos\theta), \tag{72}$$

$$g(\theta) = \frac{1}{(1-\cos\theta)^{m_2}}\sum_{l\geq 1}b_l^{(m_2)}P_l^1(\cos\theta). \tag{73}$$

The recurrence relations satisfied by the Legendre polynomials $P_l(x)$, $P_l^1(x)$ lead to the iterative rules giving the reduced coefficients in any order,

$$a_l^{(i+1)} = a_l^{(i)} - \frac{l+1}{2l+3}a_{l+1}^{(i)} - \frac{l}{2l-1}a_{l-1}^{(i)}, \tag{74}$$

$$b_l^{(i+1)} = b_l^{(i)} - \frac{l+2}{2l+3}b_{l+1}^{(i)} - \frac{l-1}{2l-1}b_{l-1}^{(i)}, \tag{75}$$

if we start with $a_l^{(0)}=a_l$ and $b_l^{(0)}=b_l$ as defined by Eqs. (52), (53) and (38). Note that in this last equation we replace $s\to\Re s-i|\Im s|$ in order to cover automatically the two cases of interest here, elastic collision and absorption. Then we will see that this method is very effective, ensuring the convergence of the reduced series for any value of θ apart from the singularity in $\theta=0$. Here we present the numerical results obtained by using the second iteration for f ($m_1=2$) and the first one for g ($m_2=1$), which seems to be satisfactory without distorting the analytical results.

In this approach the elastic and total cross sections cannot be calculated since their series remain divergent under any conditions because of the mentioned singularity. Even if we replace the amplitudes f and g with their reduced series we cannot ensure the convergence since then we introduce additional factors of the type $(1-\cos\theta)^{-n}$, $n\geq 2$, leading to divergent integrals over θ when we calculate σ_e as in Eq. (64). Therefore, we are able to study only the absorption cross section (69), which is given by

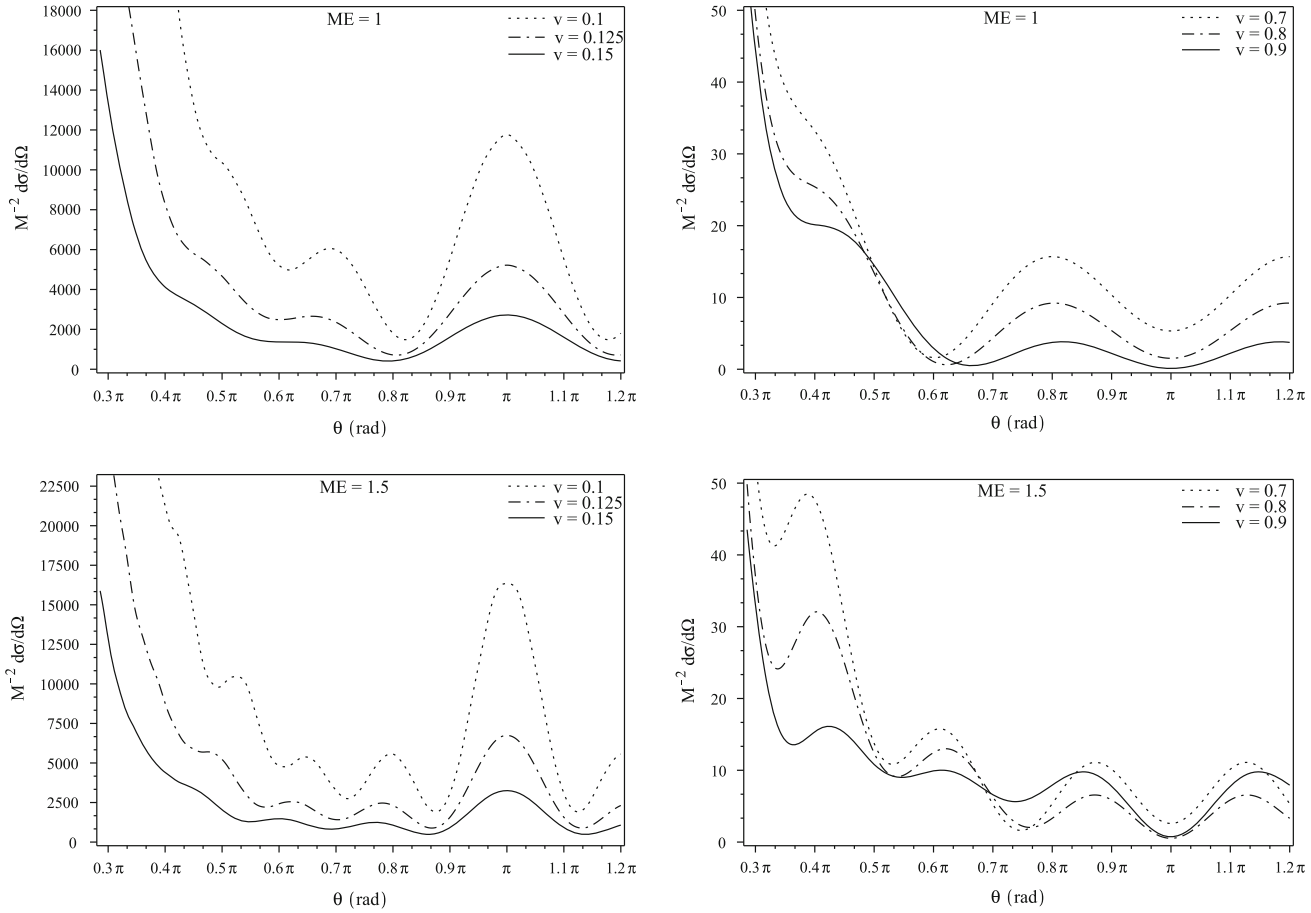

Fig. 1 The differential cross section as a function of θ for different values of the fermion speed

a finite sum, followed then by focusing on the scattering amplitudes, the scattering intensity, and the polarization degree.

All these quantities depend on three free parameters: the fermion mass m and momentum p, and the black hole mass M. Since we work in the asymptotic zone where the fermion energy is $E = \sqrt{m^2 + p^2}$, we can use the fermion velocity $v = p/E$ as an auxiliary parameter. With these parameters one can construct two relevant dimensionless quantities, which in the usual units read $GME/(\hbar c^3)$ and $mGM/(\hbar c)$. The last one can be seen as (proportional to) the ratio of the black hole horizon to the fermion Compton wavelength. In our natural units (with $c = \hbar = G = 1$) these quantities appear as ME, respectively, mM, these being used for labeling our graphs.

We should mention that our graphical analysis is performed in the following only for the case of small or micro black holes, for which ME and mM take relatively small values, since in this manner we can compare our results with those obtained by using analytical–numerical methods [22–26]. However, our analytical results presented above are valid for any values of these parameters.

4.1 Forward and backward scattering

We begin the graphical analysis by plotting the differential cross section (54), as a function of the angle θ for different numerical values of mM and ME. Since $E = \sqrt{m^2 + p^2}$, the condition $ME \geq mM$ must be always satisfied. In addition, multiplying by M the expression of energy we obtain $mM = ME\sqrt{1 - v^2}$, which gives the connection between the pair of parameters that define our analytical formulas. The graphs in Figs. 1 and 2 show how the scattering intensity depends on the scattering angle for small/large fermion velocities. In order to observe the oscillations in the scattering intensity around $\theta = \pi$, corresponding to backward scattering, we shorten the axis of θ because the cross section is divergent in $\theta = 0$.

In Figs. 1 and 2 we observe the presence of a maximum in scattering intensity in the backward direction. This is known as glory scattering [42], while the oscillations in the scattering intensity at intermediate scattering angles, around $\theta = \pi$, are known as orbiting or spiral scattering [42]. Another important observation that emerges from these graphs is that the scattering intensity has large values only for small fermion

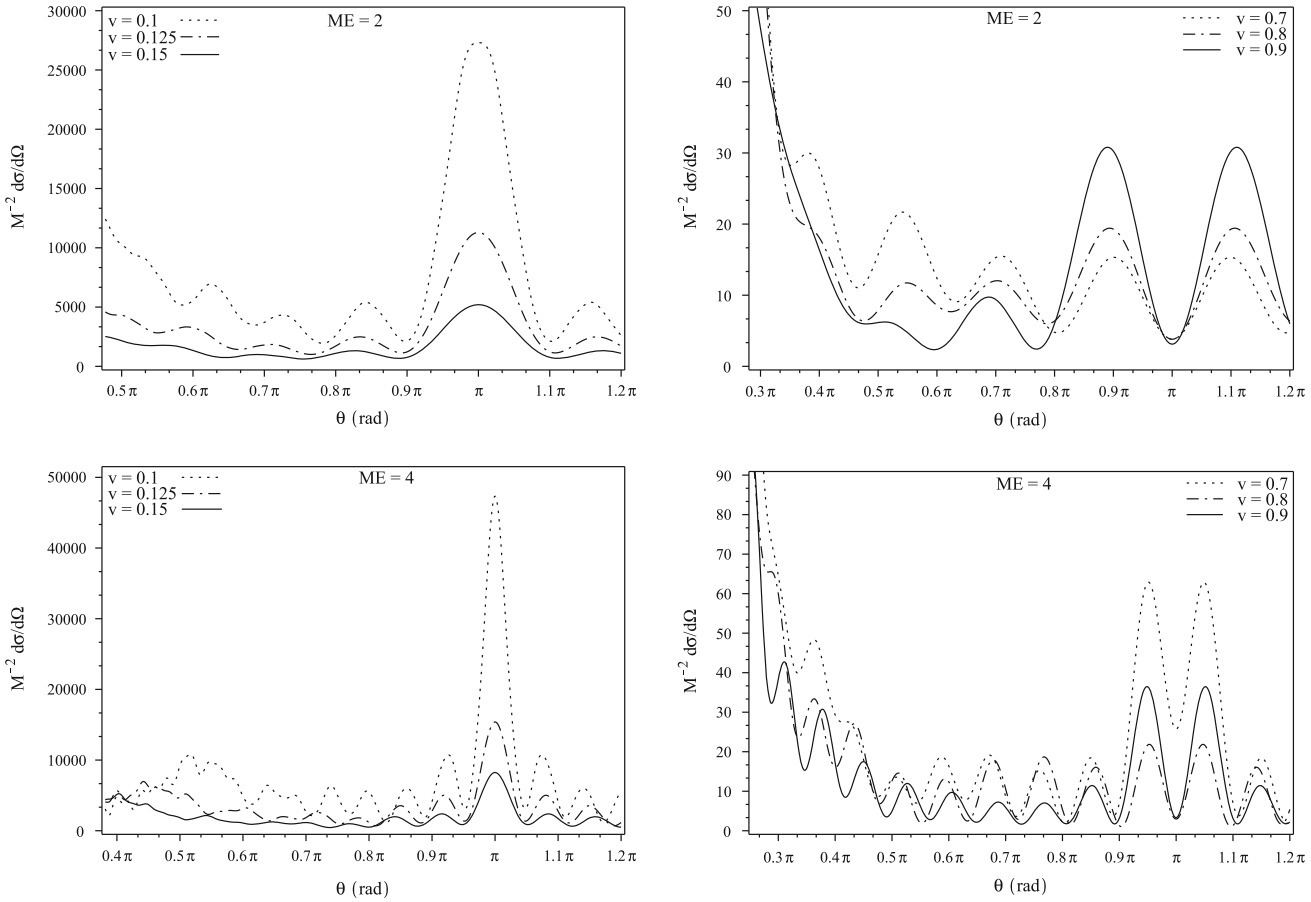

Fig. 2 The differential cross section as a function of θ for different values of the fermion speed

velocities, while at large ones the scattering intensity is observably smaller. The conclusion is that the glory and orbiting scattering are significant only for non-relativistic fermions.

At $\theta = 0$ the scattering intensity becomes divergent for both small or large values of the fermion speed. For this reason, in order to obtain the behavior of scattering intensity at small scattering angles for different fermion velocities, we restrict ourselves only to values of θ close to 0.

Our graphs in Fig. 3 show that the scattering intensity becomes divergent as $\theta \to 0$ (forward scattering) and they also show the presence of oscillations around small values of θ, i.e. the orbiting scattering [42]. We also observe that the scattering intensity in the forward direction increases with the parameter ME. The forward scattering is in fact a diffraction on the black hole horizon. This could be possible only in the case when the wavelength of the incident particle is comparable with the size of the event horizon. From Fig. 3 we observe that the oscillatory behavior of scattering intensity in the forward direction is more pronounced in the case of small fermion velocities comparatively with the case of relativistic ones. It is also worth to mention that the oscillatory behavior of the scattering intensity is increasing with the parameter ME (see Fig. 4). The conclusion is that the orbiting scattering is negligible for relativistic particles, while in the case of particles with small velocities this phenomenon becomes important.

Furthermore, we address the problem of variation of the cross section with the black hole mass given in Fig. 4. We observe that the scattering intensity in the backward direction is increasing with the black hole mass but without changing its general profile. This suggests that the positions of the relative extremes are independent on the black hole mass.

Let us comment now on the results of the scattering intensities obtained in graphs Figs. 1, 2, 3, and 4. One knows that the differential cross section represents the area that the incident particle must cross in the target zone in order to be detected in the solid angle dΩ. In the case of a scattering process between two quantum objects this quantity is very small. So in our case it is not surprising that the differential cross section becomes very large, since the target is of the size of the black hole event horizon. This can be better understood if we recall the result from classical physics according to which

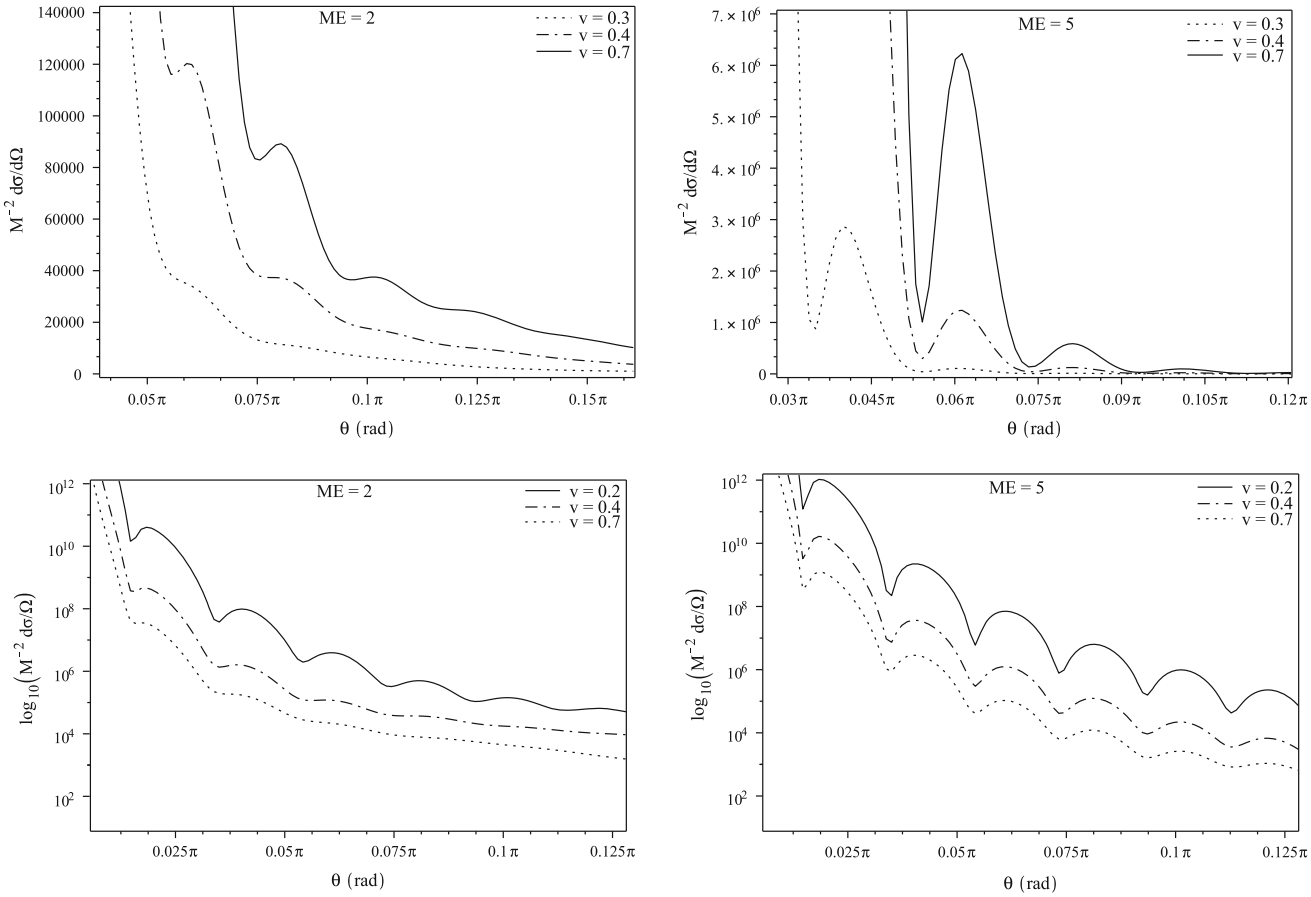

Fig. 3 The differential cross at small θ, for different values of the fermion speed

the scattering intensity for a classical particle moving on a spiral trajectory is larger that the scattering intensity for a particle moving on a straight line. A classical particle which has nonzero angular momentum will always cross a larger area in the target zone. The situation is the same in the case of a quantum particle scattered by a black hole but with the observation that in this case the notion of trajectory is not well defined. Taking into consideration that the minimum area of the target is of the size of the event horizon we see that the area crossed by the fermion to be detected in a solid angle could be very large. As a final remark we can observe that the scattering intensity in the forward/backward direction increases with the black hole mass. This result is expected since the area of the event horizon also increases with the black hole mass. Our results are compatible with those obtained in the literature using analytical–numerical methods [26].

4.2 Dependence on energy

We study now the behavior of the differential cross section in terms of the energy by plotting Eq. (54) as a function of the ratio E/m for different scattering angles. Since for $\theta = 0$ the differential cross section is divergent, our analysis is done for $\theta = \pi/3,\ \pi/4$.

Another observation that emerges from Figs. 5 and 6 is that the energy dependence of scattering intensity has a more pronounced oscillatory behavior for small scattering angles and large values of mM. On the other hand, we also observe from Figs. 5 and 6 that the scattering intensity is decreasing when the energy increases and becomes divergent in the limit of small energies. The shapes of these graphs are the result of the fact that our scattering intensity is proportional with the usual factor $1/E^2$ and the oscillatory effect is given by the more complicated dependence of the energy on the phase shift given by Eq. (38).

4.3 Polarization degree

If we consider that the fermions from the incident beam are not polarized, then after the interaction with the black hole, the scattered beam could become partially polarized. It is interesting to study this effect by plotting the degree of polarization (55) as a function of scattering angle for given values of ME and different fermion velocities. Plotting the polar-

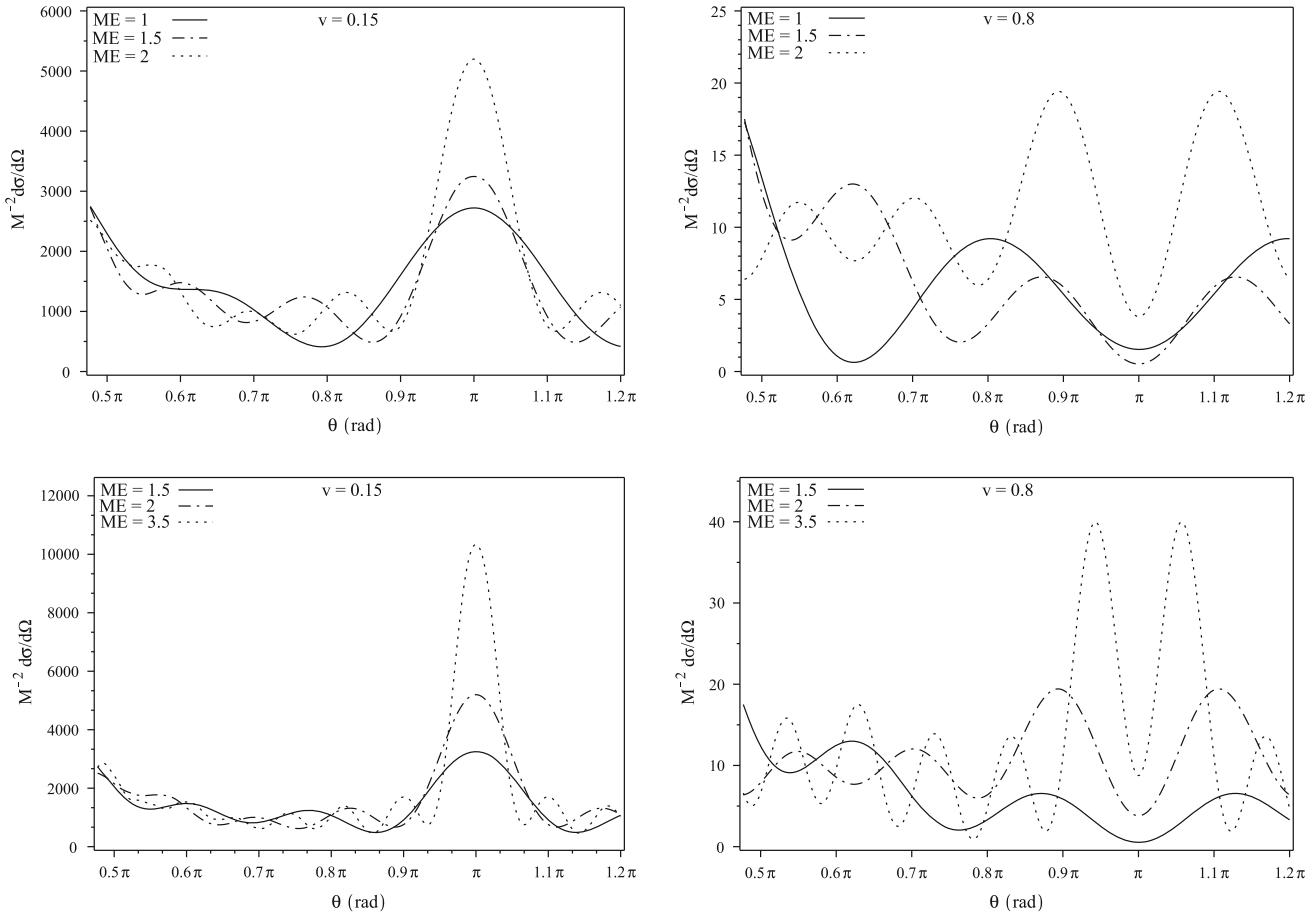

Fig. 4 The differential cross section as a function of θ for different ME at fixed values of the fermion speed

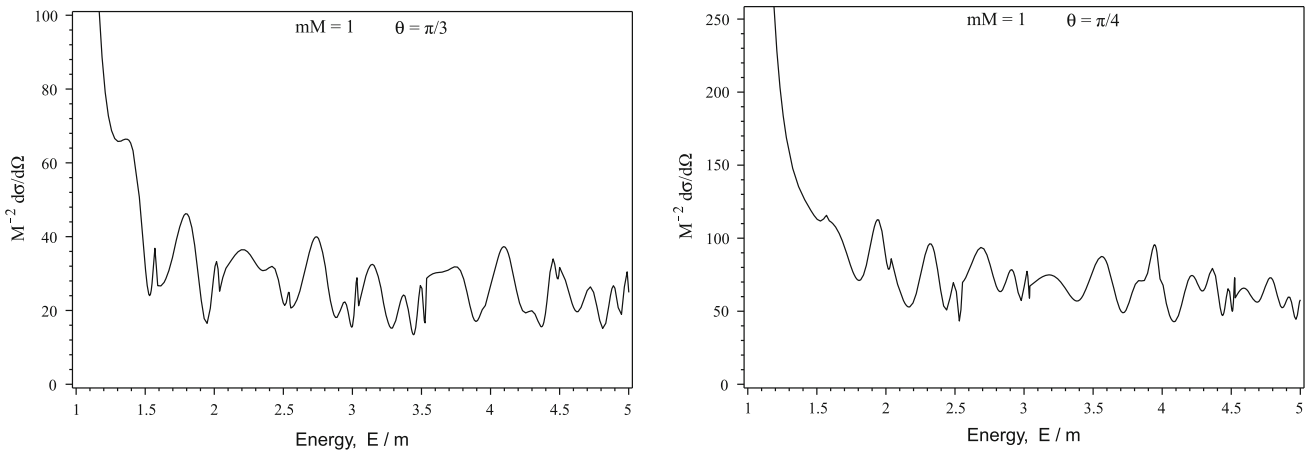

Fig. 5 Differential cross sections dependence of energy for different scattering angles and $mM = 1$

ization as a function of the scattering angle we obtain the results given in Figs. 7 and 8.

As we may observe from Figs. 7 and 8, the polarization is a very oscillatory function of the scattering angle. These oscillations are the result of the forward and backward scattering as well as the orbiting scattering. These three types of scattering induce the oscillatory behavior of polarization, since the scattering intensity also oscillates with the scattering angle. Another result that is worth mentioning is the oscillatory behavior of the polarization, Figs. 7 and 8, which

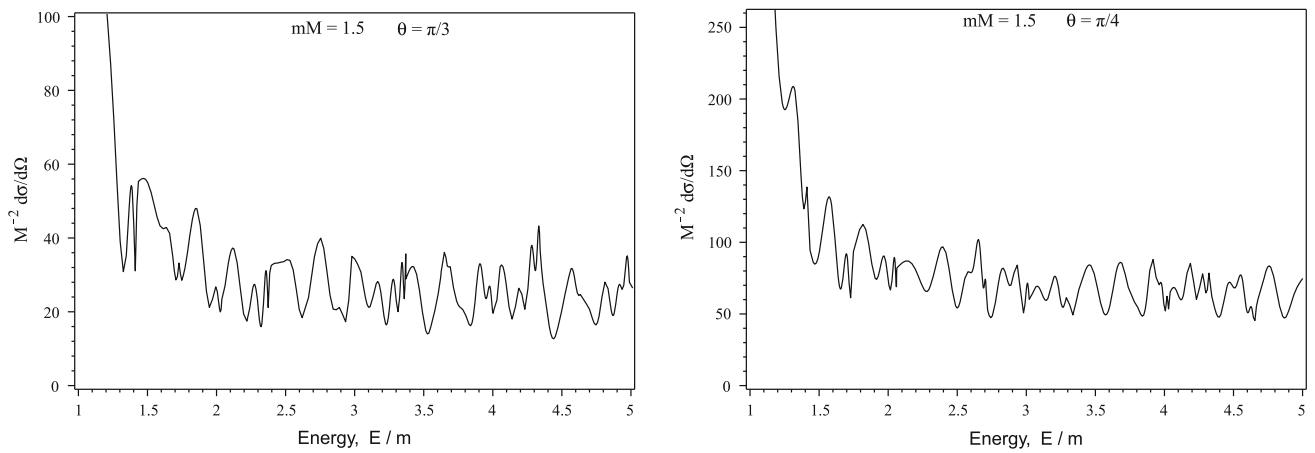

Fig. 6 Differential cross sections dependence of energy for different scattering angles and $mM = 1.5$

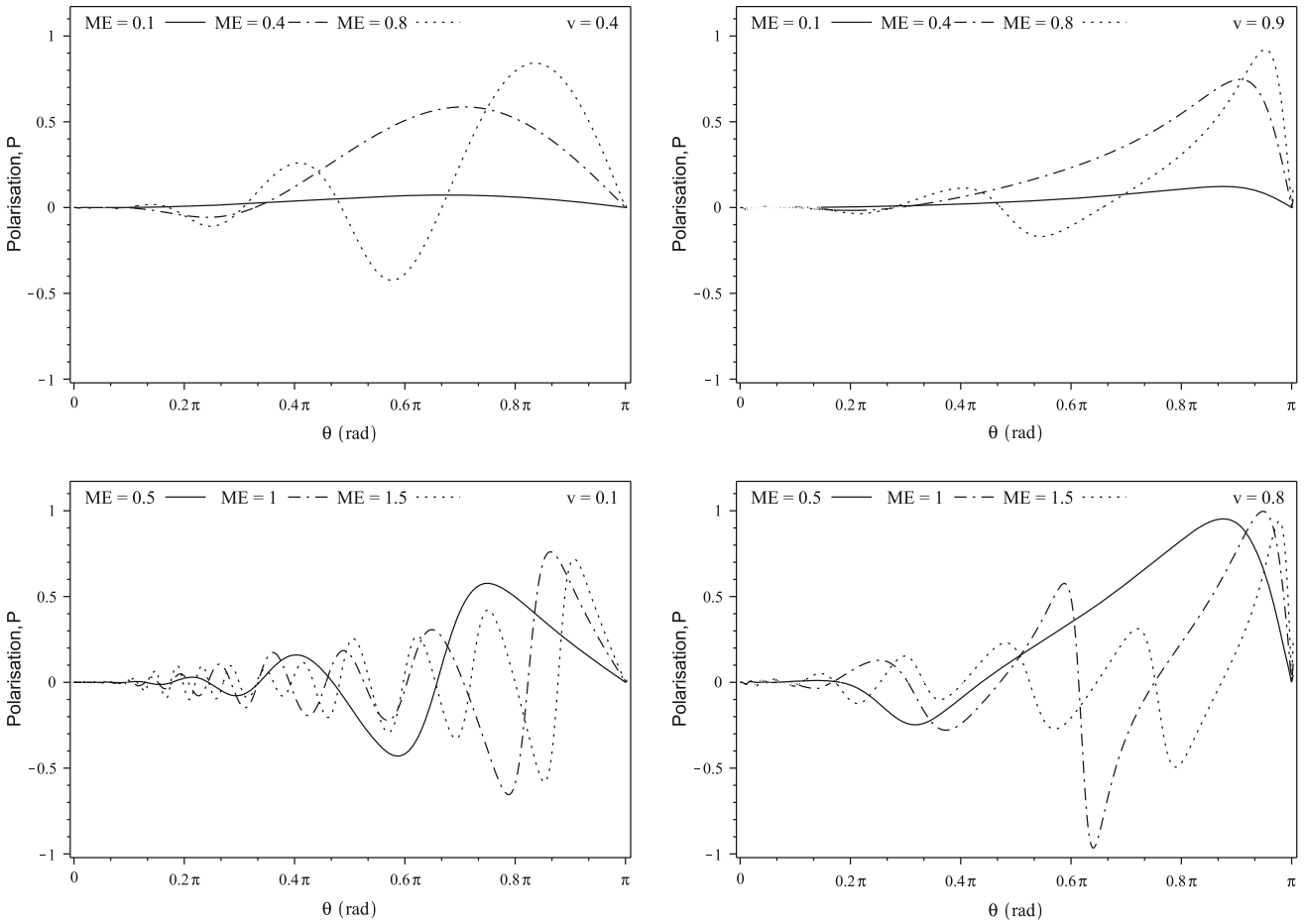

Fig. 7 The polarization degree dependence of θ for different fermion velocities

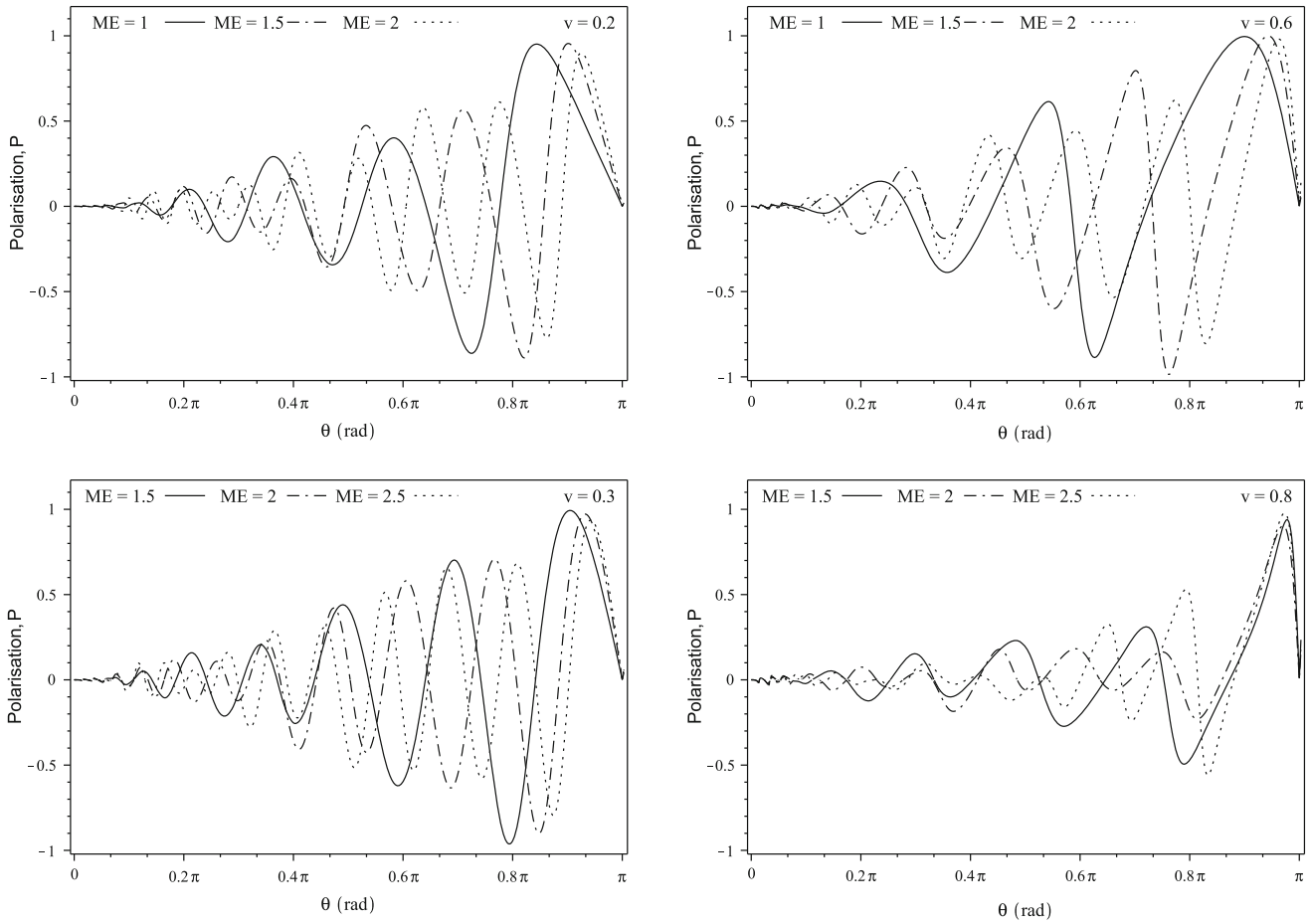

Fig. 8 The polarization degree dependence of θ for different fermion velocities

is modified as we change the parameter ME. If the fermion energy is fixed, then we can draw the conclusion that the oscillatory behavior of the polarization depends on the black hole mass M, becoming more pronounced as we increase the black hole mass.

To see how the spin of the fermion is aligned with a given direction after scattering off a black hole, we present the polar plots for the degree of polarization in Figs. 9, 10. These graphs are plotted for different values of ME and different velocities.

From our Figs. 9 and 10 we observe that the scattered wave can be partially polarized in the direction orthogonal to the scattering plane. This phenomenon is similar to the Mott polarization [43], which appears in the electromagnetic scattering. This conclusion was also underlined in Ref. [26].

4.4 Absorption cross section

The above examples show that our analytical approach reproduces correctly all the results concerning the elastic scattering obtained by using analytical–numerical methods [25,26]. However, there are significant differences in what concerns the partial absorption cross sections (69) or the total one (68).

We specify first that in our case the partial waves $|S_{-\kappa}| = |S_\kappa|$ give the *same* contribution to the partial absorption cross sections. As observed in Sect. III.B., when $\sqrt{3}mM < 1$ all these partial sections remain finite in $E = m$ as we can see in the left side of Fig. 11. However, if this quantity becomes larger than 1, then the partial sections $\sigma_a^l(p)$ with $1 < l < \sqrt{3}mM$ reach the singularity point $E = m$ where these are divergent, as in the right side of Fig. 11, where only $\sigma_a^1(p)$ becomes singular. Thus the profile of $\sigma_a(p)$ is strongly dependent on the parameter mM, as shown in Fig. 12. In the first panel (Fig. 12) we plot the cross section $\sigma_a(p) = \sigma_a^1(p)$ given by $|S_{-1}| = |S_1|$, which are the only contributions in the energy range under consideration. The next panels show the profiles of the absorption cross sections for different values of mM, pointing out the mentioned effect of the singularity in $E = m$ and the asymptotic behavior resulting from Eq. (71).

We note that the analytical–numerical results obtained so far [25,26] are somewhat different from the analytical ones we present here. The first difference is that one obtains numerically $|S_{-\kappa}| \neq |S_\kappa|$ such that the quantity

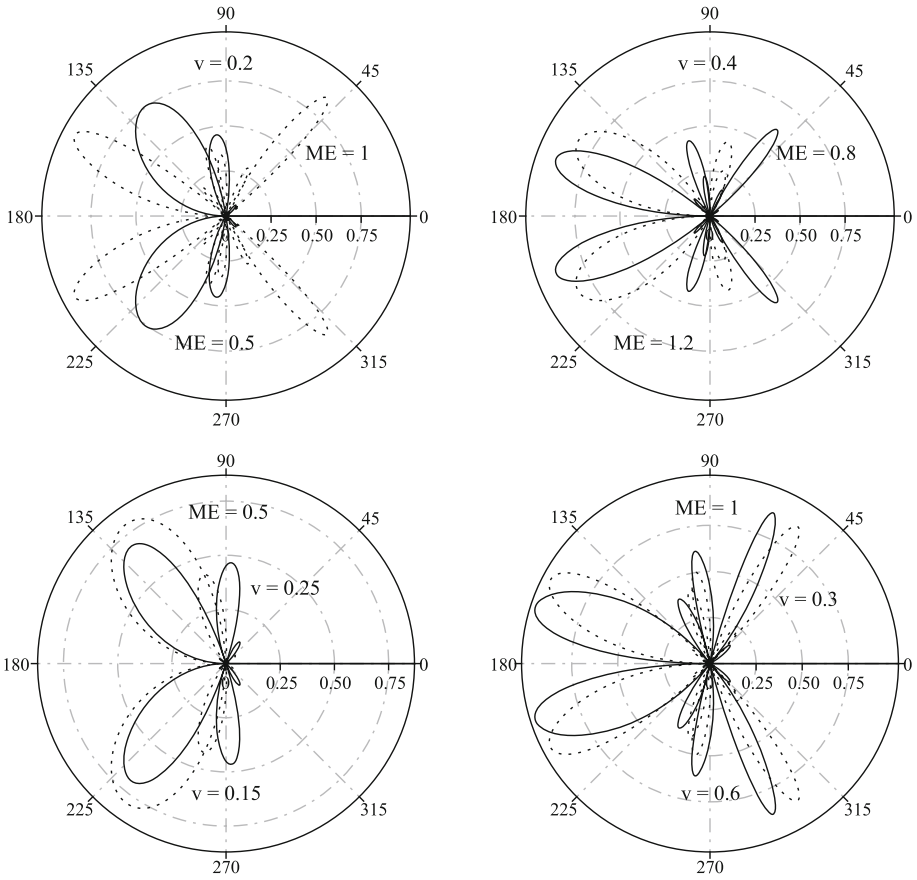

Fig. 9 Polar plot of $\mathcal{P}(\theta)$ for different values of ME and fermion velocities

$\sigma_a^{-\kappa}(p) - \sigma_a^{\kappa}(p)$ is maximal for $|\kappa| = 1$—when σ_a^{-1} (with $l = 0$) diverges for $E \to m$ while $\sigma_a^{1}(p)$ remains finite—vanishing then rapidly with increasing $|\kappa|$ [25]. The second difference is the numerical asymptote that corresponds to the geometrical photon value $27\pi M^2$, while in our case this asymptote (71) is much smaller. On the other hand, despite these two discrepancies, there are notable similarities as the general profile of the cross sections and the values of the thresholds of the partial waves become equidistant for $m = 0$.

Under such circumstances it seems that something is missing in our analytic approach, namely a possible resonant scattering that may be dominant in the s wave (with $l = 0$) and increases the absorption cross section significantly; this could explain satisfactorily the differences discussed above.

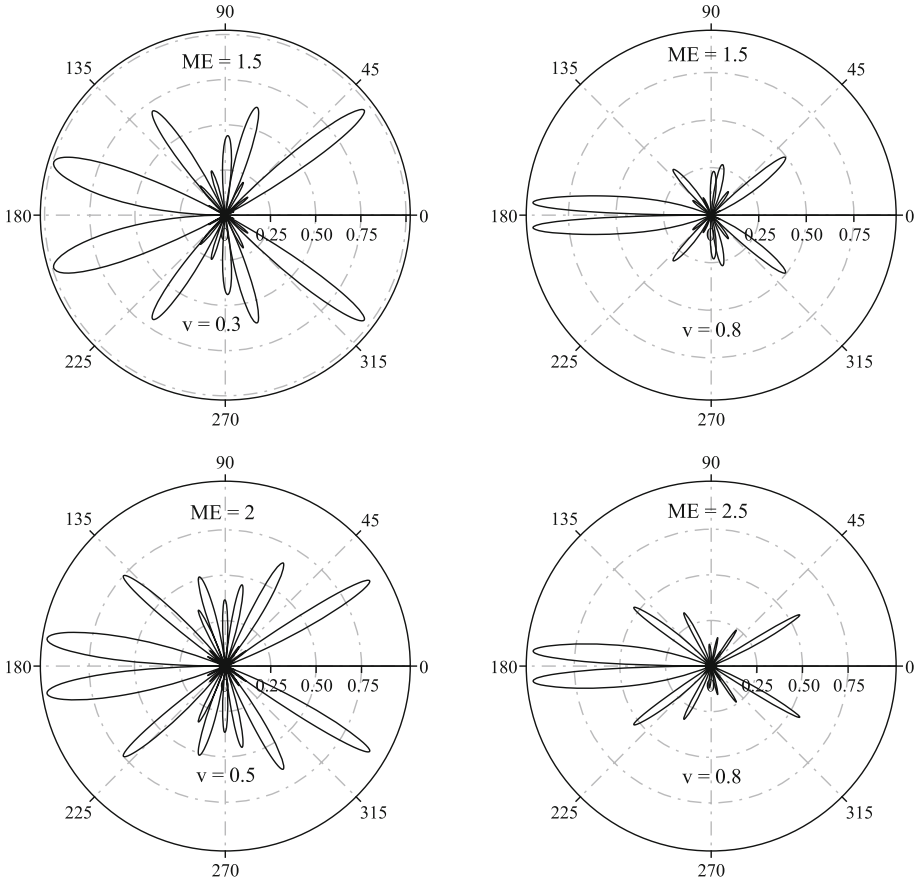

Fig. 10 Polar plot of $\mathcal{P}(\theta)$ for different values of ME and fermion velocities

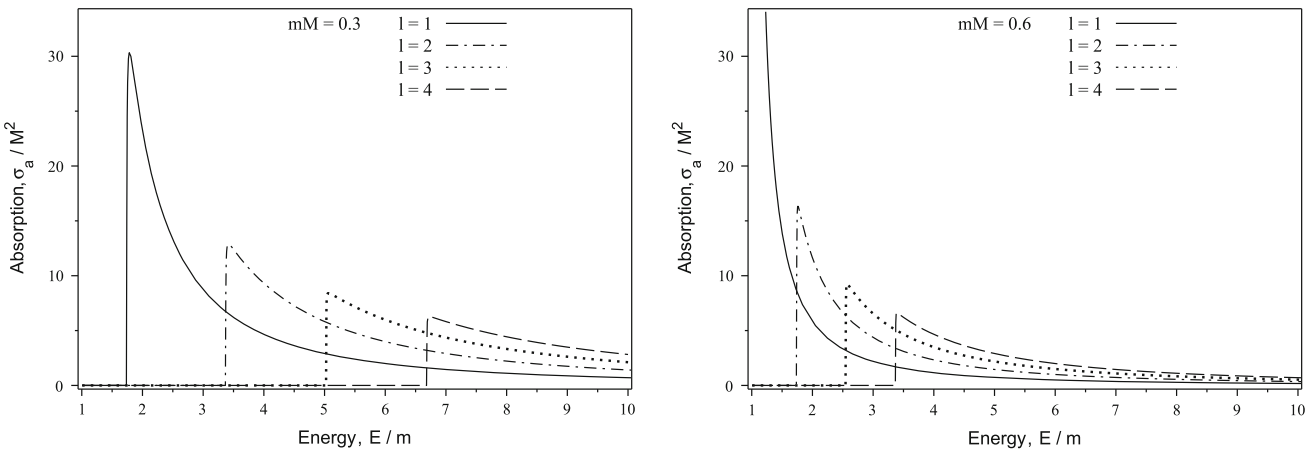

Fig. 11 Partial absorption cross sections as functions of the energy for different values of mM

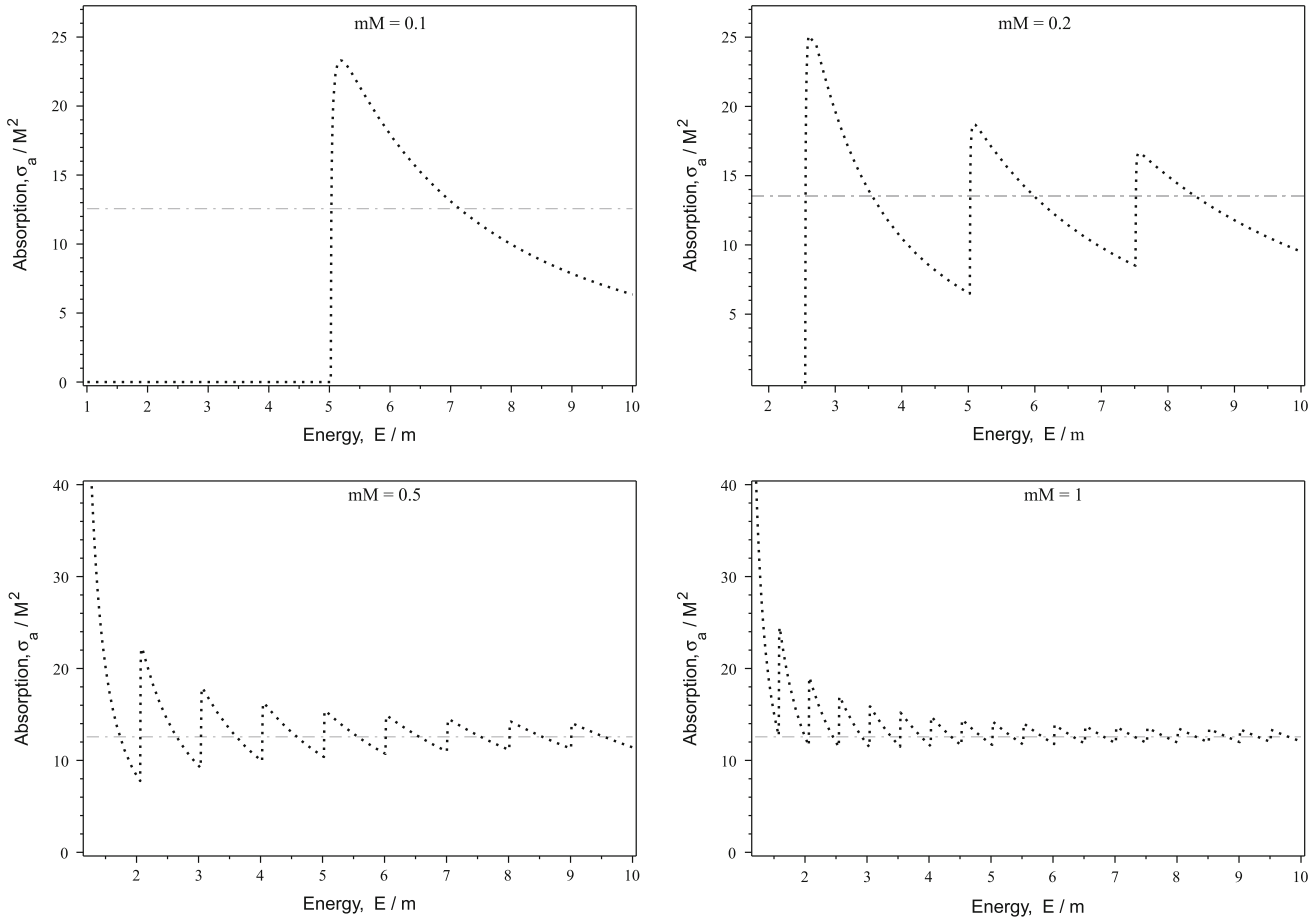

Fig. 12 Absorption cross sections as functions of energy for different values of mM

5 Concluding remarks

In this paper we performed the partial wave analysis of Dirac fermions scattered by black holes by using the approximative analytical scattering modes of the Dirac equation in Schwarzschild's charts with Cartesian gauge. Selecting a suitable asymptotic condition we obtained the analytical expression of the phase shifts that allow us to derive the scattering amplitudes, differential cross sections, and degrees of polarization. These depend on a parameter (s) that takes real values in elastic collisions, becoming pure imaginary when the fermion is absorbed by a black hole. Thus by using the same formalism we can study the elastic scattering and absorption deriving the closed form of the absorption cross section produced by the scattering modes.

From our analytical and graphical results we established that the spinor wave can be scattered in forward and backward directions and that the spiral scattering (orbital scattering) is present in both these cases. The scattering intensity in both forward and backward directions is increasing with the black hole mass. Also the oscillations in the scattering intensity around $\theta = \pi$ become more pronounced as the black hole mass is increasing. The polarization degree has an oscillatory behavior in terms of the scattering angle and depends on the black hole mass too. Our polar plots for the polarizations show what the directions are in which the spin is aligned after the interaction. We note that thanks to our analytical formulas the graphical analysis can be performed for any values of the parameters mM, ME, and v, leading to similar conclusions.

The general conclusion is that our formalism is suitable for describing the elastic fermion–black hole collisions for which we recover the entire phenomenology pointed out by analytical–numerical methods [22–26].

Acknowledgments I.I. Cotaescu and C. Crucean were supported by a grant of the Romanian National Authority for Scientific Research, Programme for research-Space Technology and Advanced Research-STAR, project nr. 72/29.11.2013 between Romanian Space Agency and West University of Timisoara. C.A. Sporea was supported by the strategic grant POSDRU/159/1.5/S/137750, Project Doctoral and Postdoctoral programs support for increased competitiveness in Exact Sciences research cofinanced by the European Social Found within

the Sectorial Operational Program Human Resources Development 2007–2013.

Funded by SCOAP[3].

Appendix A: Whittaker functions

The Whittaker functions M [40] have the property

$$M_{-\kappa,\mu}(-z) = e^{i\pi(\mu+\frac{1}{2})} M_{\kappa,\mu}(z), \tag{A1}$$

and the asymptotic representation for large $|z|$,

$$M_{\kappa,\mu}(z) \sim \frac{\Gamma(1+2\mu)}{\Gamma(\frac{1}{2}+\mu-\kappa)} e^{\frac{1}{2}z} z^{-\kappa} \left(1+O(z^{-1})\right) + e^{i(\frac{1}{2}+\mu-\kappa)\pi} \frac{\Gamma(1+2\mu)}{\Gamma(\frac{1}{2}+\mu+\kappa)} e^{-\frac{1}{2}z} z^{\kappa} \left(1+O(z^{-1})\right), \tag{A2}$$

which holds in the case of our radial functions where $-\frac{1}{2}\pi < \mathrm{ph}\, z = \frac{\pi}{2} < \frac{3}{2}\pi$.

Appendix B: Newtonian limit

In the case of scalar particles scattered from black holes, the phase shifts δ_l^N in the large-l limit satisfy [20,21]

$$e^{2i\delta_l^N} = \frac{\Gamma(1+l-iq)}{\Gamma(1+l+iq)}. \tag{B1}$$

where q is given by Eq. (41). Then the partial amplitudes,

$$f_l^N = \frac{1}{2ip}\left(e^{2i\delta_l^N} - 1\right), \tag{B2}$$

can be expanded as

$$f_l^N = -M\frac{\beta}{p^2} + iM^2\frac{\beta^2}{p^3} + O(M^3), \qquad \beta = (2p^2+m^2)\psi(l+1). \tag{B3}$$

Appendix C: Condition of elastic scattering

Let us consider the problem of the appropriate asymptotic conditions determining the integration constants of the solutions (26) and (27), which satisfy Eq. (29). It is convenient to introduce the new notation (up to a real arbitrary common factor)

$$C_1^+ = e^{i\theta_1}, \quad C_2^+ = Ce^{i\theta_2}, \qquad C_1^- = e^{\theta_1}\frac{s-iq}{\kappa-i\lambda}, \quad C_2^- = -\frac{C}{\kappa-i\lambda}e^{i\theta_2}, \tag{C1}$$

where C, θ_1, and θ_2 are real-valued parameters. Then, according to Eq. (A1), we obtain the general asymptotic representation for large $|z|$, of our solutions,

$$\hat{f}^+ \sim e^{iv^2x^2}(2v)^{\frac{1}{2}+iq}x^{2iq}e^{-\frac{1}{2}\pi q}e^{i\theta_1}\frac{\Gamma(1+2s)}{\Gamma(1+s+iq)},$$
$$\hat{f}^- \sim e^{iv^2x^2}(2v)^{\frac{1}{2}-iq}x^{2iq} \times \left[e^{\frac{1}{2}\pi q}e^{i\pi s}e^{-\pi q}e^{i\theta_1}\frac{s-iq}{\kappa-i\lambda}\frac{\Gamma(1+2s)}{\Gamma(1+s-iq)} - C\frac{e^{i\theta_2}e^{\frac{1}{2}\pi q}}{\kappa-i\lambda}\right].$$

These solutions can be put in the trigonometric form (33) where the argument is given by $\frac{1}{2}\arg\frac{f^+}{f^-}$, as mentioned before in Sect. 3.1. Then by using the method indicated therein we deduce the general expression of the phase shifts,

$$e^{2i\delta_\kappa} = \frac{\kappa-i\lambda}{s+iq}\frac{\frac{\Gamma(1+2s)}{\Gamma(s+iq)}e^{i\pi(l-s)}}{\frac{\Gamma(1+2s)}{\Gamma(s-iq)} - Ce^{i\theta}e^{-i\pi(s+iq)}}, \tag{C2}$$

with arbitrary integration constants, which holds for any value of the parameter s, which can take either real values, $s = |s|$, or pure imaginary ones, $s = \pm i|s|$. We observe that the phase shifts depend now only on the two real integration constants C and the relative phase $\theta = \theta_1 - \theta_2$.

The elastic scattering can arise only when we have

$$\left|e^{2i\delta_\kappa}\right| = 1. \tag{C3}$$

There are two cases. In the first one, when $s = |s|$, Eq. (C3) has two real solutions, $C = 0$ and

$$C = e^{-\pi q}\frac{\Gamma(1+2s)}{|\Gamma(s+iq)|^2} \times \left[e^{i(\pi s-\theta)}\Gamma(s+iq) + e^{-i(\pi s-\theta)}\Gamma(s-iq)\right]. \tag{C4}$$

The second case is of pure imaginary $s = \pm i|s|$ when the above equation has no real solutions.

Furthermore, we observe that the phase shifts have the correct Newtonian limits (B1) for large l only if we choose the asymptotic condition $C = 0$ (i.e. $C_2^+ = C_2^- = 0$) when the phase shifts are completely determined, being given by Eq. (38). Otherwise, if we consider the solution (C4) we obtain non-determinate phase shifts,

$$e^{2i\delta_\kappa} = -\frac{\kappa-i\lambda}{s+iq}e^{i(\pi l+\pi s-2\theta)}, \tag{C5}$$

which are still depending on the arbitrary phase θ. Obviously, in this case we cannot speak about the Newtonian limit.

The conclusion is that we must consider the asymptotic condition $C = 0$ giving the correct phase shifts in elastic collisions for $s = |s|$. However, it is natural to keep the same condition for $s = \pm i|s|$ when the collision is no longer elastic because of the absorption of the fermions by a black hole.

References

1. R.A. Matzner, J. Math. Phys. (N.Y.) **9**, 163 (1968)
2. R. Fabbri, Phys. Rev. D **12**, 933 (1975)
3. P.C. Peters, Phys. Rev. D **13**, 775 (1976)
4. W.K. de Logi, S.J. Kovacs, Phys. Rev. D **16**, 237 (1977)
5. N.G. Sanchez, J. Math. Phys. (N.Y.) **17**, 688 (1976)
6. N.G. Sanchez, Phys. Rev. D **16**, 937 (1977)
7. N.G. Sanchez, Phys. Rev. D **18**, 1030 (1978)
8. N.G. Sanchez, Phys. Rev. D **18**, 1798 (1978)
9. T.R. Zhang, C. DeWitt-Morette, Phys. Rev. Lett. **52**, 2313 (1984)
10. R.A. Matzner, C. DeWitt-Morette, B. Nelson, T.R. Zhang, Phys. Rev. D **31**, 1869 (1985)
11. P. Anninos, C. DeWitt-Morette, R.A. Matzner, P. Yioutas, T.R. Zhang, Phys. Rev. D **46**, 4477 (1992)
12. N. Andersson, Phys. Rev. D **52**, 1808 (1995)
13. N. Andersson, B.P. Jensen, arXiv:gr-qc/0011025
14. C.J.L. Doran, A.N. Lasenby, Phys. Rev. D **66**, 024006 (2002)
15. S. Chandrasekhar, *The mathematical theory of black holes* (Oxford University Press, New York, 1983)
16. V.P. Frolov, I.D. Novikov, *Black hole physics: basic concepts and new developments* (Kluwer Academic Publishers, Dordrecht, 1998)
17. J. Chen, H. Liao, Y. Wang, Eur. Phys. J. C **73**, 2395 (2013)
18. D. Batic, N.G. Kelkar, M. Nowakowski, Eur. Phys. J. C **71**, 1831 (2011)
19. D. Batic, N.G. Kelkar, M. Nowakowski, Phys. Rev. D **86**, 104060 (2012)
20. J.A.H. Futterman, F.A. Handler, R.A. Matzner, *Scattering from black holes* (Cambridge University Press, Cambridge, 1988)
21. N.K. Kofiniti, Int. J. Theor. Phys. **23**, 991 (1984)
22. J. Jing, Phys. Rev. D **70**, 065004 (2004)
23. J. Jing, Phys. Rev. D **71**, 124006 (2005)
24. K.H.C. Castello-Branco, R.A. Konoplya, A. Zhidenko, Phys. Rev. D **71**, 047502 (2005)
25. C. Doran, A. Lasenby, S. Dolan, I. Hinder, Phys. Rev. D **71**, 124020 (2005)
26. S. Dolan, C. Doran, A. Lasenby, Phys. Rev. D **74**, 064005 (2006)
27. I.I. Cotăescu, Mod. Phys. Lett. A **22**, 2493 (2007)
28. I.I. Cotăescu, J. Phys. A Math. Gen. **33**, 1977 (2000)
29. B. Thaller, *The Dirac equation* (Springer Verlag, Berlin, Heidelberg, 1992)
30. I.I. Cotăescu, Mod. Phys. Lett. A **13**, 2923 (1998)
31. I.I. Cotăescu, Mod. Phys. Lett. A **13**, 2991 (1998)
32. I.I. Cotăescu, Phys. Rev. D **60**, 124006–010 (1999)
33. I.I. Cotăescu, Int. J. Mod. Phys. A **19**, 2217 (2004)
34. I.D. Novikov, Doctoral disertation, Sthernberg Astronomical Institute (1963)
35. C.W. Misner, K.S. Thorne, J.A. Wheeler, *Gravitation* (Freeman & Co., San Francisco, 1971)
36. A. Lasenby, C. Doran, J. Prithchard, A. Caceres, S. Dolan, Phys. Rev. D **72**, 105014 (2005)
37. V.B. Berestetski, E.M. Lifshitz, L.P. Pitaevski, *Quantum electrodynamics* (Pergamon Press, Oxford, 1982)
38. W.G. Unruh, Phys. Rev. D **14**, 3251 (1976)
39. I.I. Cotăescu, Phys. Rev. D **60**, 124006 (1999)
40. F.W.J. Olver, D.W. Lozier, R.F. Boisvert, C.W. Clark, NIST handbook of mathematical functions (Cambridge University Press, 2010)
41. D.R. Yennie, D.G. Ravenhall, R.N. Wilson, Phys. Rev. **95**, 500 (1954)
42. K.W. Ford, G.A. Wheeler, Ann. Phys. **7**, 259 (1959)
43. N.F. Mott, H.S.W. Massey, *The theory of atomic collisions* (Oxford University Press, London, 1965)